Regenerative Therapy 24 (2023) 85–93

Contents lists available at ScienceDirect

Regenerative Therapy

journal homepage: http://www.elsevier.com/locate/reth

Original Article

# Neural regeneration ability of Polypyrrole-Collagen-Quercetin composite in the spinal cord injury

Song Zhang [a, 1], Qifeng Li [a, 1], Song Zhang [b, *]

[a] Department of Neurosurgery, Hangzhou Children's Hospital, Hangzhou Normal University, Hangzhou City, Zhejiang Province, China
[b] Department of Neurosurgery, The Second Affiliated Hospital of Guizhou University of Traditional Chinese Medicine, Guiyang City, Guizhou Province, China

ARTICLE INFO

*Article history:*
Received 14 March 2023
Received in revised form
22 May 2023
Accepted 28 May 2023

*Keywords:*
Antioxidant
Electrical conductivity
Collagen
Quercetin
Spinal cord regeneration

ABSTRACT

Spinal cord injury (SCI) is a major clinical problem in young patients. The major hurdle in SCI regeneration is the replacement of lost nerve communication signals due to injury. Here we have prepared a biocompatible electrical conductive composite such as Collagen-Polypyrrole combined with Quercetin (Col-PPy-Qur) composite. The prepared composites are characterized for their chemical functionality and morphology by the FTIR and SEM & TEM analysis, respectively. The Col-PPy-Qur composite observed electrical conductivity at 0.0653 s/cm due to the conductive Polypyrrole polymer present in the composite. The Col-PPy-Qur composite exhibits a mechanical strength of 0.1281 mPa, similar to the native human spinal cord's mechanical strength. In order to explore the regeneration potential, the viability of the composite has been tested with human astrocyte cells (HACs). The Tuj1 and GFAF marker expression was quantized by RT-PCR analysis. Increased Tuj1 and decreased GFAF expression by the Col-PPy-Qur composite indicated the potential differentiation ability of the HACs into neuron cells. The results indicated that the Col-PPy-Qur composite could have good regeneration and differentiation ability, better biocompatibility, and suitable mechanical and conductivity properties. It can act as an excellent strategy for spinal cord regeneration in the nearer future.
© 2023, The Japanese Society for Regenerative Medicine. Production and hosting by Elsevier B.V. This is an open access article under the CC BY-NC-ND license (http://creativecommons.org/licenses/by-nc-nd/4.0/).

## 1. Introduction

Spinal cord injury (SCI) is caused by damage to the axons that present along the spinal cord, resulting in motor, sensory and autonomic nerve function below the injury site [1]. Specifically, SCI affects young male patients majorly through traumatic injuries. The lifetime expenses of patients with SCI exceed $3 million per individual, depending on the level of injury [2]. The long-term disability of patients with SCI becomes a psychological and economic burden. However, no appropriate treatment for SCI has been demonstrated, and various pieces of research are in progress. Stem cell-based therapies have attained much interest in treating SCI as they have significant potential in saving damaged tissues and inducing functional nerve recovery [3]. The drawbacks of using stem cells, such as ethical controversies and risks of developing tumors, have limited the applications in regeneration therapies [4]. In addition to the drawbacks mentioned above, there is a lack of physical support to maintain the mechanical strength of the native spinal cord.

Biomaterials, as a basic platform for tissue engineering, provide physical support to the axons to grow along the scaffold, promote functional recovery after SCI and have been widely used in SCI repair. Biomaterial scaffolds can also be used as a carrier for cells and drugs to control the diffusion rate in the injury site [5]. Biomaterial scaffolds can be prepared with Natural or synthetic materials depending on the need. Natural polymers like Collagen (Col), Hyaluronic acid, Chitosan, Gelatin, Agarose, Alginate, and Fibrin have been used to prepare biomaterial scaffolds in SCI regeneration research as they have good biocompatibility, biodegradability [6]. Col is the majorly found protein in the human body, responsible for forming various tissues, organs, and it is widely used in drug delivery and tissue engineering applications [7,8]. The advantages of Col include excellent biodegradability, biocompatibility, osteocompatibility, good cell adhesive properties, and weak

* Corresponding author.
*E-mail address:* zhangsong121988@sina.com (S. Zhang).
Peer review under responsibility of the Japanese Society for Regenerative Medicine.
[1] Song Zhang and Qifeng Li are co-first authors, Song Zhang and Qifeng Li have contributed equally to this work.

https://doi.org/10.1016/j.reth.2023.05.010
2352-3204/© 2023, The Japanese Society for Regenerative Medicine. Production and hosting by Elsevier B.V. This is an open access article under the CC BY-NC-ND license (http://creativecommons.org/licenses/by-nc-nd/4.0/).

antigenicity. In addition, Col can form strong fibers with superior stability when cross-linking network formation [7,8]. Hence, Col-based biomaterial scaffolds attained the researcher's interest in biomedical applications. S. Liu et al., in 2020 demonstrated a hindlimb functional recovery after SCI in a rat model using neural stem cells loaded multi-channel conduit Col scaffolds. The Col scaffolds were prepared by the freeze-drying method using multi-channel conduit mold. The prepared scaffolds showed good biocompatibility and biodegradability and promoted nerve regeneration [5].

Zhang et al. (2021) prepared paclitaxel (PTX) loaded exosome-Col scaffolds for SCI repair. They have demonstrated that exosome-derived human umbilical cord mesenchymal stem cells can promote the migration of endogenous neural stem cells, and PTX can induce neuronal growth. The prepared multifunctional scaffold has shown excellent performance for functional recovery after SCI in rats by inducing neuronal regeneration [9]. Yin Liu et al. (2021) developed a brain-derived neurotrophic factor (BDNF) loaded Col/Chitosan scaffold by low-temperature 3D printing. It demonstrated significant functional recovery after eight weeks of implantation in a rat model [10].

The spinal cord transfers the electrical nerve signals between the brain and the organs of the body. As SCI damages, the spinal cord leads to the disruption in nerve signals. Studies have shown that reimbursing the disturbed nerve signal helps regenerate the injury and improve functional recovery after SCI [11–15]. Hence, scientists have been working with conductive materials to develop SCI regeneration research. Conducting materials like conducting polymers, carbon materials, and metal nanoparticles have been subjected to use in SCI treatment. Conducting polymers like Polypyrrole (PPy), polyaniline, and poly (3,4-ethylene dioxythiophene) have attained much interest [16].

In 2018, Zhou et al. synthesized a soft conducting hydrogel composed of PPy and tannic acid with conductivity and mechanical stability similar to the native spinal cord [17]. The *in-vitro* studies have shown the hydrogel's excellent ability to differentiate the neural stem cells into neurons with suppression of astrocytes. The high conductivity of the hydrogel has induced endogenous neurogenesis and helps in the functional recovery of SCI rat models. Raynald et al., in 2019, prepared a bone marrow stromal cell (BMSC) loaded nanofibrous scaffold composed of PPy and polylactic acid (PLA) by electrospinning technique. *In-vivo* tests were conducted randomly in three Sprague-Dawley rats groups: control group, PPy/PLA group, and PPy/PLA/BMSCs group. Compared with other groups, excellent functional recovery with inhibited scar formation was found in PPy/PLA/BMSCs group [18]. Wu et al., in 2021, developed a conductive hydrogel with antioxidant properties for SCI repair. The prepared PPy nanoparticles have been shown to exhibit excellent antioxidant effects along with appropriate conductivity. The PPy nanoparticles have been incorporated into the hydrogel made with Col and hyaluronan. The bone marrow mesenchymal stem cells loaded with conductive hydrogel showed outstanding nerve regeneration and functional recovery in the rat model [19].

Followed by primary injury, secondary injury causes a series of oxidative, inflammatory reactions in the injury site, inhibiting the regeneration process. Flavonoids are a special class of natural products with antioxidant, anti-inflammatory, and neuroprotective properties and have been widely used in SCI treatment [20]. Qur's anti-inflammatory and antioxidant properties have attained particular interest in SCI therapy [21]. Schultke et al. has investigated the therapeutic effects of Qur against SCI in Wistar rat models. The results have demonstrated that Qur administration induces functional recovery after 4 weeks [21]. Wang et al., in 2017, have demonstrated that Qur administration can induce astrocyte activation, axonal regeneration, and functional recovery in rat models [22]. Keeping these factors in mind, we have prepared a Qur-loaded electrical conductive composite composed of Col and PPy for spinal regeneration investigation.

## 2. Materials and methods

### 2.1. Materials

Collagen (Col) (Marine fish extract), Quercetin (Qur), Dimethyl sulfoxide (DMSO)were obtained from Sigma Aldrich, China. Polypyrrole (PPy) was obtained from Sigma Aldrich, China. All chemicals were obtained from analytical grade and were used as purchased without further purification. Double-distilled (DD) water was used throughout the experiments.

### 2.2. Synthesis of Col-PPy composite

The previously published procedure followed the Col-PPy composite preparation with slight modifications [23]. Briefly, 50 mg of Col was dissolved in 0.1 M acetic acid solution, and 50 mg of PPy was added to the Col solution. The Col-PPy blende was prepared by simply mixing Col with PPy with a ratio of 1:1 and then stirred in a magnetic stirrer for 8 h at room temperature (25 °C). After the stirring completion, the Col-PPy composite was lyophilized (Lyomac Lyopro-1 Lyophilizer, LYORPO-1, China) at −40 °C for 24 h. The prepared Col-PPy composite chemical functionality changes and morphology were characterized.

### 2.3. Synthesis of Col-PPy-Qur composite

Quercetin was loaded into the Col-PPy composite, followed by the previous report by the simple stirring method [24]. Briefly, the 10 mg of Qur was dissolved in Dimethyl sulfoxide (DMSO) and added into 100 mg of Col-PPy composite in an acetic acid solution. At room temperature, the reaction mixture was kept in a magnetic stirrer for 12 h. The DMSO and acetic acid solvents were removed from the resulting Col-PPy-Qur composite by solvent evaporation technique [25]. Further, the composite was lyophilized (Lyomac Lyopro-1 Lyophilizer, LYORPO-1, China) at −40 °C for 24 h. The schematic representation for the formation of Col-PPy-Qur composite was given in the Scheme 1.

### 2.4. Physiochemical characterizations

#### 2.4.1. Fourier transformed infrared spectroscopy (FT-IR)

Fourier transform infrared spectroscopy (IRTRACER-100, SHIMADZU) was used to detect the chemical functional groups of Col, Col-PPy, and Col-PPy-Qur composites. These prepared composites were mixed with a certain amount of KBr to make a tablet form, which was scanned in the spectral region of 400–4000 $cm^{-1}$.

#### 2.4.2. X-ray diffraction analysis (XRD)

The X-ray diffraction (XRD) interpretation was carried out to break down the stage arrangement and get the crystallinity of the synthesized Col-PPy-Qur composite. The XRD investigation was practiced in a Bruker D8 Advance Diffractometer with a monochromatic Cu Kα source worked at 40 kV and 30 mA. A stepping-up voltage of 30 kV and a current of 15 mA were applied. The working scope of the determination was over the 2θ territory from 10 to 60° in sync check mode with a stage size of 0.02° and a sweeping pace of 0.02°/min.

#### 2.4.3. Electron microscopic analysis

The surface morphology of the prepared Col, Col-PPy, and Col-PPy-Qur composites was examined through SEM by operating it

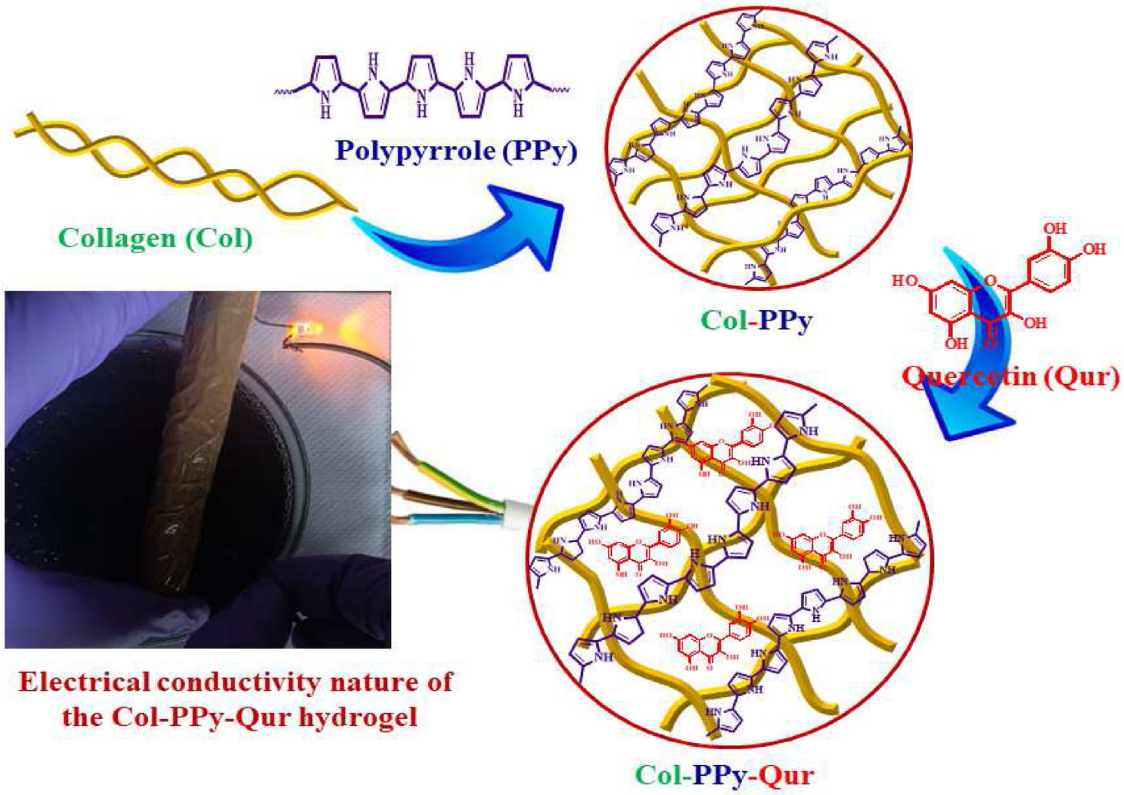


**Scheme 1.** Schematic representation of Col-PPy-Qur composite and their electrical conductivity nature by illumination of LED light.

at an extent voltage of 10 kV. The samples were prepared by dispersing the sample in DD water, whereas the materials were examined by SEM (VEGA3 TESCAN). TEM images of the Col-PPy-Qur composite were analysed with FEI Technai G220 S- TWIN TEM by dropping the dispersed samples on a copper grid.

*2.4.4. Thermogravimetric analysis (TGA)*

Thermal gravimetric analysis (TGA) was measured on Shimadzu-TA 60 instrument with a heating rate of 25 °C $min^{-1}$ using crucibles aluminum under an $N_2$ atmosphere.

*2.4.5. Conductivity analysis*

The electrical conductivity of the prepared samples was analysed by Four Probe Method. Resistance was measured and then converted into conductivity using the below equation,

$$\text{Conductivity} = V/I\ (2\pi S)$$

V is the voltage, I is the current, and S is the distance between the probes.

*2.4.6. Stress-strain measurements*

The measurements of stress-strain parameters were done by carrying out the solidity tests with a universal testing machine (Shimadzu, AGS-J, Japan). The Col-PPy-Qur composite was shaped into cylinders (~7 mm in length and ~7 mm in diameter). The sample was condensed at a 90-degree angle to the cross-section of the cylinders with a crosshead speed of 0.5 mm $min^{-1}$. This experiment was carried out three times, and the mechanical strength was determined by the initial linear portion slope of the stress-strain curve and expressed as the mean values.

*2.5. Biological characterizations*

*2.5.1. Cell culture*

We bought human astrocyte cells (HACs) from Thermo Fisher Scientific, China, that were generated from the rat cerebral cortex. Using an astrocyte complete growth medium (821-500, Thermo Fisher Scientific, China), cells were cultivated and kept at 37 °C in a $CO_2$ incubator (95% air, 5% $CO_2$). The cells were passaged by trypsinization using trypsin/EDTA once they had attained 80–90% confluency (ThermoFisher Scientific, USA). For 24 h, the human astrocytes were exposed to various concentrations of newly produced composites.

*2.5.2. Cell viability*

The viability and Proliferation of the cells were assessed using an MTT assay (Cat # ab211091, Abcam, UK). In 96-well plates, cells were cultivated at a density of around 103 cells per well, and when they had attained 90% confluency, the cells were treated. The treatment media and 50 μL of the serum-free medium were removed 24 h after the start of the treatment, and 50 μL of MTT reagent was added to each well. 50 μL of MTT reagents and 50 μL of cell culture media (without cells) were put into the background control wells and included for 3 h at 37 °C. The MTT reagent was then removed, 150 μL of MTT assay was supplemented into each well, the plate was covered with foil, and the plate was shaken for 30 min in an orbital shaker. The absorbance was determined using a UV-Visible spectrophotometer at the $\lambda_{max}$ value of 590 nm.

*2.5.3. Hoechst 33258 staining*

The morphology of HACs on different composites at different concentrations was assessed by staining nuclei with Hoechst 33258

(bisbenzimide trihydrochloride) (Invitrogen, H21491, ThermoFisher Scientific, China). After 12, 24, and 48 h incubation on composites, the cells were washed with PBS thrice and incubated with Hoechst 33258 (10 μg/mL) of 5% $CO_2$ at 37 °C in an atmosphere for 7 min. Cells were again washed thrice with PBS to remove excess dye and viewed under a Carl Zeiss Axio Observer Z1 fluorescence microscopy (352Ex/461 Em).

#### 2.5.4. Osteogenic differentiation by gene expression studies

Gene expression research on neurogenic differentiation Real-time polymerase chain reaction analysis of mRNA levels was used to determine cell phenotypic (RT-PCR). After being cultured for 14 days, the samples were washed three times in PBS before being placed in cold TRIzol Reagent (1 mL). Using the conventional TRIzol technique, the total RNA of each sample was extracted and then re-deposited in RNase-free water (50 L) [26]. The cDNA was produced according to the procedure and kept at −20 °C until further examination. The PCR was quantitatively analysed using a power SYBR green RT-PCR kit methodology, and the experiments were carried out in triplicate (n = 3). The genes Tuj1 (β-tubulin III, a cytoskeletal marker unique to neurons) and GFAP (glial fibrillary acidic protein) were used as neuronal markers. Control cells were those that had not been treated. Table 1 contains a list of the primer sequences that were utilized.

### 2.6. Statistical evaluation

The information is displayed as the standard error of the mean (SEM). The SPSS 24.0 program was used to assess statistical differences between groups.

## 3. Results and discussion

### 3.1. FTIR analysis

FTIR spectra of Col, Col-PPy, and Col-PPy-Qur composite have been analysed, and results are presented in Fig. 1. The FTIR of the spectrum of Col shows all the characteristic peaks of collagen polymer (Fig. 1a) [27]. Amide I, II, and III bands at 1658 $cm^{-1}$, 1540 $cm^{-1}$, and 1240 $cm^{-1}$, and the peaks of NH stretching for amide bands and C–H bending vibration mode were found at 3400 $cm^{-1}$, 1451 $cm^{-1}$. In the Col-PPy composite spectrum, Col peaks and functional peaks PPy polymer were observed. The peak at 3415 $cm^{-1}$ and 1640 $cm^{-1}$ denotes the presence of Col polymer in the Col-PPy composite. The C=C stretching of PPy was attributed to the peak at 1556 $cm^{-1}$, and the peak at 1515 $cm^{-1}$ denotes the pyrrole ring stretching of the Col-PPy composite [28]. The C–H and C–N plane deformation of pyrrole was found at 1397 $cm^{-1}$ and 1186 $cm^{-1}$ [29], and these peaks confirm the formation of the Col-PPy composite. The final composite spectrum (Col-PPy-Qur) possesses the peaks corresponding to the Qur molecule peak in addition to Col, PPy components peaks shown in Fig. 1c. The peak near 3400 $cm^{-1}$ denotes the NH stretching of the amide bond of Col, and the peaks at 3428 $cm^{-1}$ and 3260 $cm^{-1}$ represent the -OH group stretching of Qur molecule. The OH bending vibration of phenol functional groups of Qur was found at 1389 $cm^{-1}$, and the carbonyl aryl ketonic stretching was found at 1680 $cm^{-1}$. The aromatic C=C

**Table 1**
The sequences primers of Tuj1 and GFAP markers.

| Gene | Forward Primer Sequences | Reverse Primer Sequences |
|---|---|---|
| Tuj1 | TCACGCAGCAGATGTTCGAT | GTGGCGCGGGTCACA |
| GFAP | CCTGAGAGAGATTCGCACTCAA | CTCCTCTGTCTCTTGCATGTTACTG |

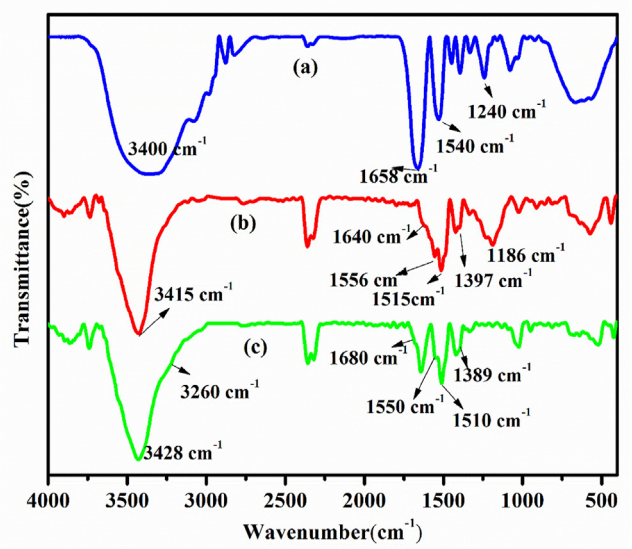


**Fig. 1.** FTIR spectra of Col (a), Col-PPy (b), Col-PPy-Qur (c) composites.

stretching was found at 1550 and 1510 $cm^{-1}$, responsible for the presence of Qur molecule in the Col-PPy-Qur composite [30]. FTIR results confirm the formation of Col-PPy and Col-PPy-Qur composite, and the structural identification and characterization are essential for materials used in medicinal applications.

### 3.2. Crystalline and thermogravimetric analysis

The crystalline phase and plane diffraction of the final composite Col-PPy-Qur was characterized using an XRD technique, and the spectrum is given in Fig. 2a. The broad diffraction peak at 20° was observed, establishing the nature of amorphous carbon. A broad hump near 22° is the characteristic peak of Col, indicating that collagen has low crystallinity [31]. A broad peak near 25° indicates the presence of PPy polymer [32]. The peak near 27° denotes the crystalline nature of the Qur molecule [33]. Moreover, the XRD spectrum of Col-PPy-Qur retained all peaks corresponding to Col, PPy, and Qur components, indicating the presence of molecules in the final composite with semi-crystalline nature.

The thermal stability of Col-PPy-Qur composite was investigated TGA under an $N_2$ atmosphere from 100 to 700 °C as given in Fig. 2b. Weight loss of the composite was observed across the entire temperature range, which can be attributed to the decomposition or weight loss of physically interacted molecules. The TGA curve of the composite exhibits three stages of weight loss. In the first step, the decomposition ranged from room temperature to 100 °C. They demonstrated the evaporation of physically observed water molecules in the composite [34]. The next steps indicated that the thermal decomposition range from 150 to 350 °C involved the removal of $CO_2$, CO, and $NO_2$ molecules from the Col-PPy-Qur composite. The degradation of the aromatic structure indicates the mass loss at 350–700 °C [35]. The thermal degradation studies indicated the composite is stable and not degraded under lower temperatures.

### 3.3. Mechanical strength and conductivity test of Col-PPy-Qur

The stress-strain curve obtained from the compressive test is shown in Fig. 3a. The modulus was calculated from the straight-line region of the stress-strain curve. The measured compressive modulus of the composite Col-PPy-Qur is 0.1281 MPa. Neuron cells

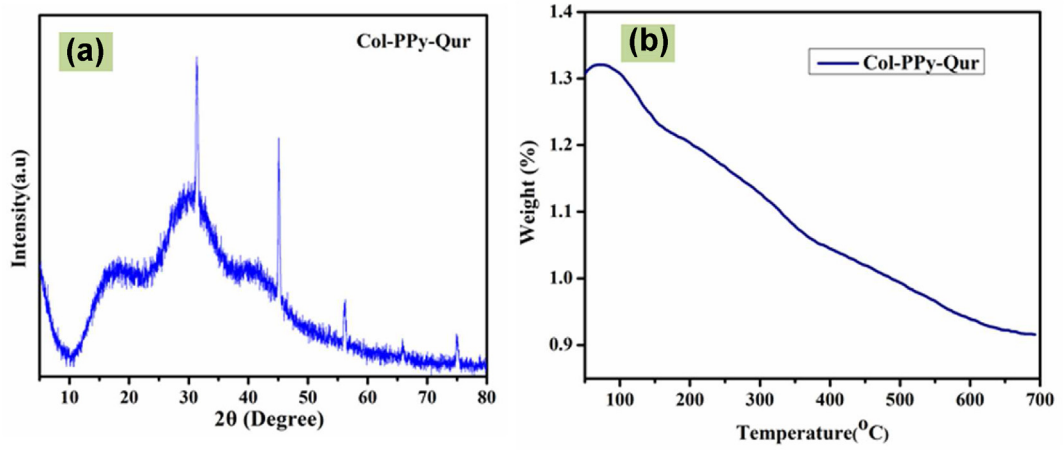


**Fig. 2.** (a) XRD spectra of Col-PPy-Qur composite, (b) TGA analysis of Col-PPy-Qur composite.

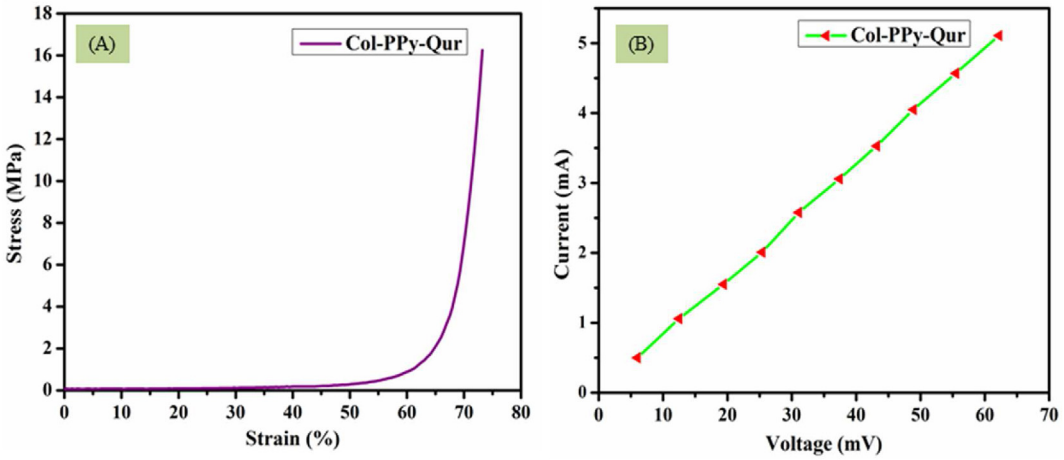


**Fig. 3.** (a) Stress-strain curve of Col-PPy-Qur composite, (b) I–V curve of Col-PPy-Qur composite.

exhibit high sensitivity to substrate stiffness during neurite outgrowth, producing relatively substantial adhesion forces and traction stresses. They exhibit maximal outgrowth on surfaces with elastic moduli of the order of 1 kPa. Strong neurite-substrate mechanical connections were thought to allow neurons to produce extremely long axons and withstand the surrounding tissue's relatively substantial external stresses [36]. Similarly, the electrical conductivity is generally accepted that the interactions between substrates and cells should be primarily governed. It implies that a Polypyrrole-based interface's tolerable range of electrical conductivity is wider than anticipated and that the atomic structure and associated surface chemistry may promote a physiological connection with the neurons [37]. The electrical conductivity of the composite Col-PPy-Qur was measured by the four-probe method. The I–V curve of the final composite is shown in Fig. 3b, with the voltage increasing linearly with increasing current, and the calculated conductivity was 0.0653 S/cm, similar to the native neural cell's electrical conductivity [12].

### 3.4. Morphological analysis

The surface morphology of the prepared composites is analysed using SEM analysis and TEM techniques. Fig. 4 shows the SEM images of (a) Col, (b) Col-PPy, (c, d) Col-PPy-Qur composites. Fig. 4a represents Col, and it shows the microporous fiber bundle-like structure. Similarly, Holder et al. prepared collagen gel for mechanical ability by controlling the manipulation of gelation near the sol–gel transition [38]. Morphological investigations are frequently used in studies of the microstructural changes related to gelation since the mechanical characteristics are among the most sensitive indicators of growing gel network microstructures [39]. A crucial step in gel formation is the development of the gel network, and recent research on fibrin gelation, which also produces a branched fiber network similar to that seen in collagen, has revealed that the mechanical/morphological characteristics of an early gel network, or the first network to span a sample, can be used to predict the structure of the mature gel [40]. Grafting of PPy in Col results in some morphological changes observed, uniform granular morphology shown in Fig. 3b. Previously, the Polypyrrole obtained a granular morphology, and the average grain size is ~0.7 μm [41]; here, the PPy was a deposit on the Col fiber. The aggregated, rough surface morphology in Fig. 4c indicates the addition of Qur in the Col-PPy composite with good interactions [42]. Hence, the composite shows scaffold-like morphology with a rough surface denoting the aggregation of PPy, Qur with Col fiber matrix that may help in cell hold to penetration, Proliferation, and axonal elongation. In addition, the morphological studies of the Col-PPy-Qur composite were observed by the TEM analysis, which is shown in Fig. 4. The dark areas throughout the particle can be observed and attributed to the Quercetin molecule present in the composite [43].

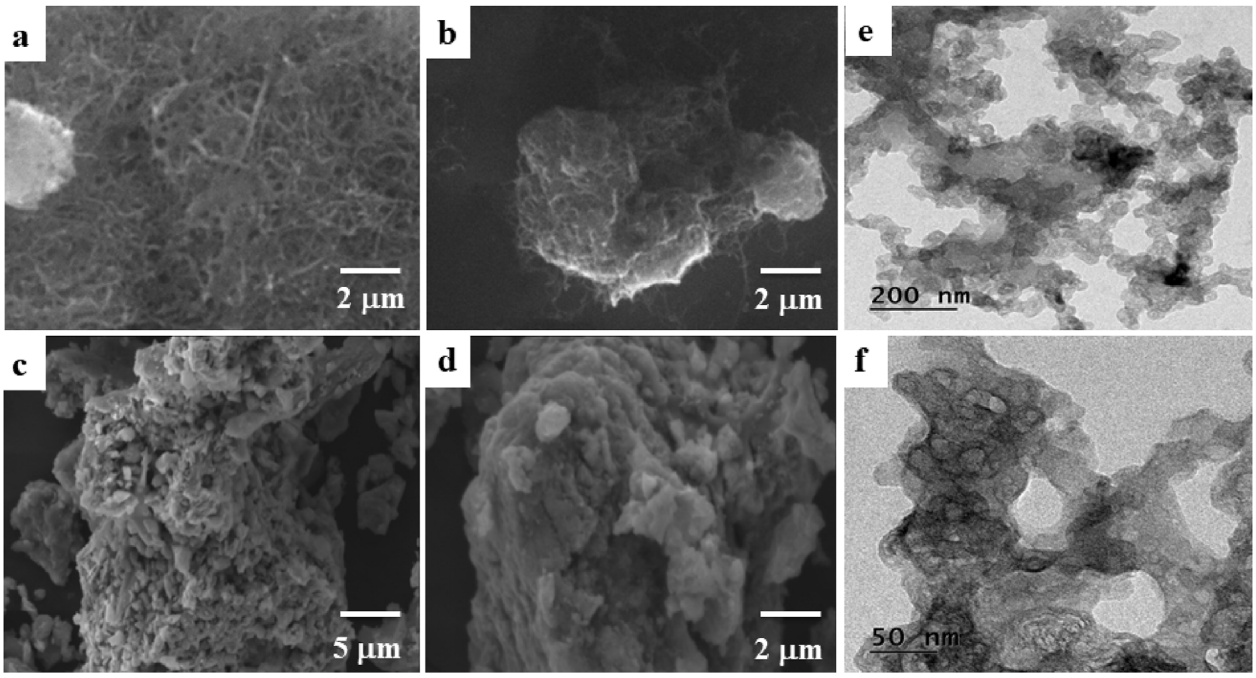


**Fig. 4.** SEM images of (a) Col, (b) Col-PPy, (c, d) Col-PPy-Qur composite, and TEM images of Col-PPy-Qur composite (e, f).

The round platelet shape indicates the presence of Polypyrrole [44]. The TEM morphology is well correlated with the SEM morphology of the Col-PPy-Qur composite.

### 3.5. Cell morphology and proliferation

The prepared Col, Col-PPy, and Col-PPy-Qur composites investigated their viability on HACs cells. The viability was increased with the increase of hours (Fig. 5). The cell viability increases with increasing time. Compared with the control, after the loading with Col and Col-PPy samples, viability was decreased. The Col-PPy-Qur composite was observed to have maximum viability compared to the other two materials and control. It is due to the Qur molecule enhancing neural regeneration properties. Quercetin can increase the ability of oxidative stress, prevent myelin sheath loss, and encourage axonal regeneration [45]. In addition, Quercetin has a crucial role in controlling the mTOR signaling pathway, which lessens the degenerative changes brought on by neuronal damage.

Quercetin's ability to protect rats' brains from the harm that high altitude might inflict on them was studied by Mehany et al. GSH, GR, GPX, GST, SOD, and CAT levels were shown to be elevated following quercetin therapy; however, MDA levels were found to be low. The study also supported Quercetin's function in treating brain injury and its capacity to scavenge free radicals produced due to

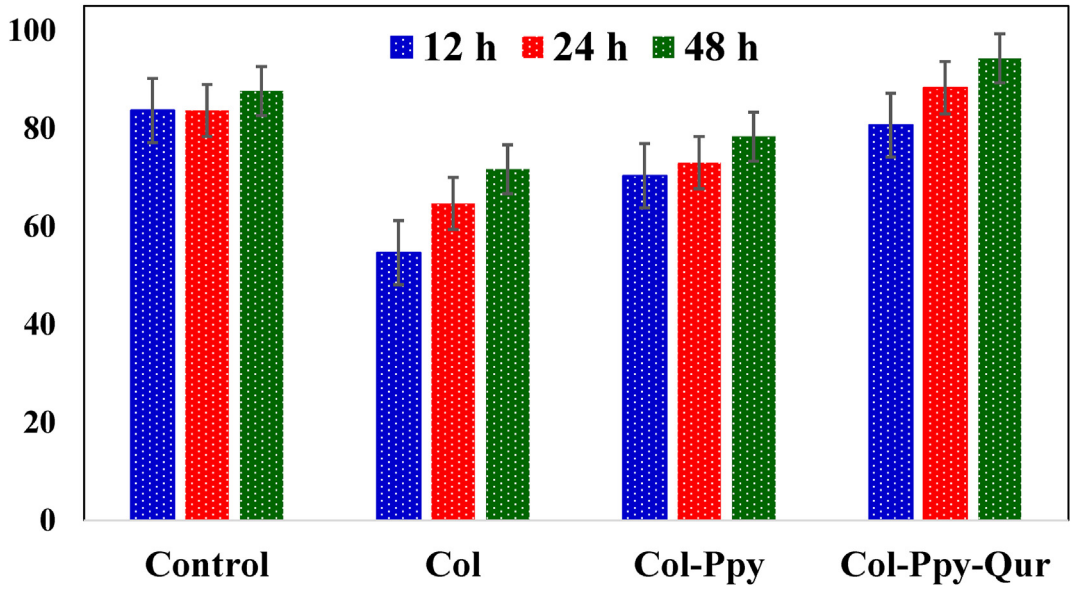


**Fig. 5.** Cell viability analysis of Col, Col-PPy, Col-PPy-Qur composites in the HACs cells.

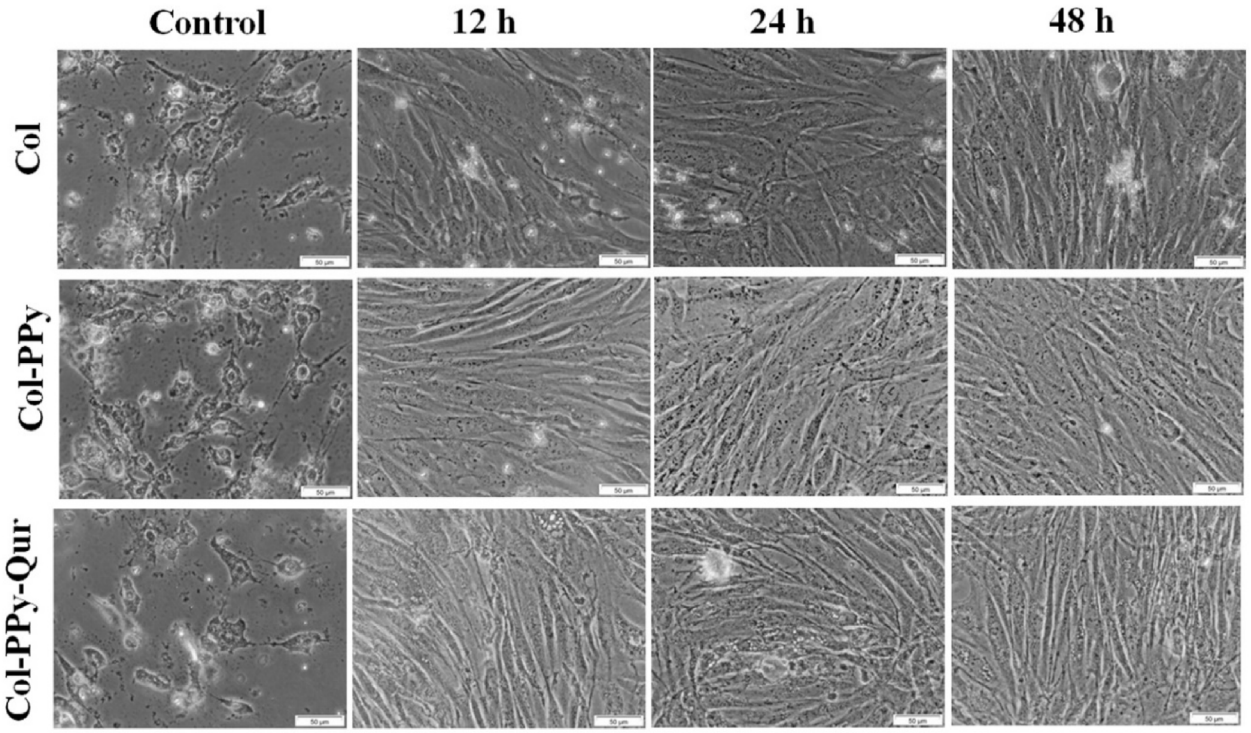


**Fig. 6.** Morphological analysis of human astrocytes in control and prepared composites for different time intervals.

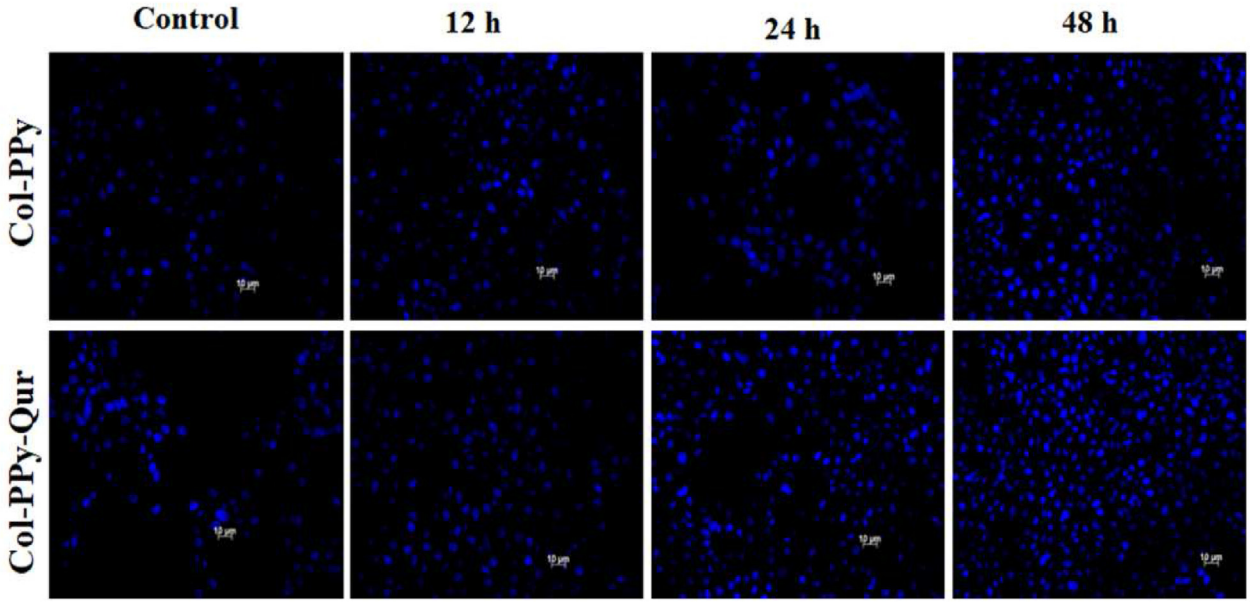


**Fig. 7.** Live cell staining of human astrocytes cells in control, Col-PPy, and Col-PPy-Qur composite for different time intervals.

hypoxia [46]. The morphological observation of the cell proliferation ability of prepared composites was analysed. Fig. 6 shows the cell morphology at different hours. When treated with Col-PPy-Qur composite, the cells showed the highest Proliferation of cells than the control and other samples. The treatment of Col-PPy-Qur composite enhances the Proliferation at 48 h compared with the other two-time hours. The cell proliferation morphology is well correlated with the cell viability results.

### *3.6. Hoechst 33258 staining live cell image*

Fig. 7 shows Hoechst 33258 staining was carried out to detect live cells in the HACs cells. The blue color indicates DAPI staining live cells, and the cell nucleus appeared circular in shape. No apoptosis was observed in the HACs cells after different hours of incubation of Col-PPy, Col-PPy-Qur composite. In these observations, the presence of Qur greatly reduced cell death after 48 h of

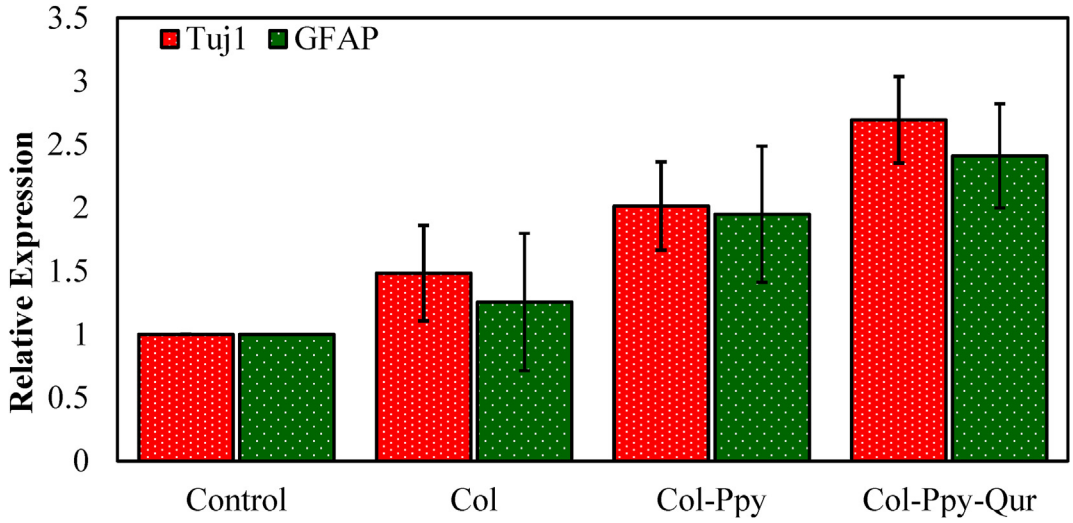


**Fig. 8.** RT-PCR analysis of Tuj1 and GFAP markers by Col, Col-PPy, Col-PPy-Qur composites.

treatment compared to the control, and a higher number of cells showed in the Col-PPy-Qur composite treated. The positive results in the compatibility of the composites arise from the biocompatibility of the polymers and their surface morphology the composites. The presence of the Qur molecule increases cell viability without producing cytotoxic effects and enhances spinal regeneration. The fabrication of a Col-PPy-Qur composite facilitates the cell viability of f HACs cells. In collective, the composite made from Col-PPy-Qur composite will act as spinal cord injury regeneration materials in further clinical applications.

### *3.7. RT-PCR analysis of neuronal markers*

RT-PCR analysis for the expression of Tuj1 mRNA (β-tubulin III, a neuronal-specific cytoskeletal marker) and GFAP mRNA (glial fibrillary acidic protein) was determined, and the results were given in Fig. 8. In newly formed immature post-mitotic neurons, differentiated neurons, and some mitotically active neural precursors, Neuron-specific class III β-tubulin (Tuj1) is present. The intermediate filaments present only in neurons are called neurofilaments. TuJ1 mRNA expression increased when Col, Col-PPy, and Col-PPy-Qur composite was treated in HACs to encourage differentiation towards a neuronal lineage, according to the results of the RT-PCR study [47]. The main intermediate filament of mature astrocytes is GFAP, and this cell type's relatively limited production of this protein suggests a critical role [48]. In addition, the decreased expression of GFAP mRNA in the Col-PPy-Qur composite confirms the increased neuronal differentiation and decreasing gliosis, and elevated GFAP protein expression in the cells [18]. Previously, Xiaofang Wu et al. discovered that at 7 days after injury, GFAP mRNA was significantly upregulated in every location [49]. This finding is in line with other earlier studies that have shown gliosis and elevated GFAP protein expression as side effects of SCI [50].

## 4. Conclusion

In conclusion, we have successfully designed and fabricated a Collagen-Quercetin-Polypyrrole composite through physical interaction. The prepared materials' chemical functionalization and surface morphology, such as Col, Col-PPy, and Col-PPy-Qur composite, were evaluated using FT-IR and SEM & TEM analysis. The synthesized composites' phase properties and thermal stability were analysed by XRD and TGA techniques. The electrical conductivity was observed at 0.0653 S/cm, similar to the electrical conductivity of human neural cells. The Col, Col-PPy, and Col-PPy-Qur composite is viable for the HACs cells. The quercetin presence induces cell differentiations, and the Tuj1 mRNA expression results also confirm cell differentiation. In the present work, we establish that the Col-PPy-Qur composite could be successfully applied as an enhancer for spinal cord injury regeneration in the nearer future.

## Data availability statement

All data generated or analysed during this study are included in this published article.

## Declaration of competing interest

The authors declare that they have no known competing financial interests or personal relationships that could have appeared to influence the work reported in this paper.

## References

[1] Alizadeh SM Dyck, Abdolrezaee SK. Traumatic spinal cord injury: an overview of pathophysiology, models and acute injury mechanisms. Front Neurol 2019;10:282.
[2] Anam A, Yazid MD, Daud MF, Idris J, Hweing AM, Rashidah Ismail ASOH, et al. Spinal cord injury: pathophysiology, multimolecular interactions, and underlying recovery mechanisms. Int J Mol Sci 2020;21(20):7533.
[3] Gao L, Peng Y, Xu W, He P, Li T, Lu X, et al. Progress in stem cell therapy for spinal cord injury. Stem Cell Int 2020;v2020:2853650.
[4] Volarevic V, Markovic BS, Gazdic M, Volarevic A, Jovicic N, Arsenijevic N, et al. Ethical and safety issues of stem cell-based therapy. Int J Med Sci 2018 Jan 1;15(1):36–45. https://doi.org/10.7150/ijms.21666.
[5] Liu S, Xie YY, Wang LD, Tai CX, Chen D, Mu D, et al. A multi-channel collagen scaffold loaded with neural stem cells for the repair of spinal cord injury. Neural Regen Res 2021;16(11):2284.
[6] Liu S, Xie YY, Wang B. Role and prospects of regenerative biomaterials in the repair of spinal cord injury. Neural Regen Res 2019:1352.
[7] Lee CH, Singla A, Lee Y. Biomedical applications of collagen. Int J Pharm 2001;221:1–22.
[8] Glowacki J, Mizuno S. Collagen scaffolds for tissue engineering. Biopolymers 2008;89(5):338–44.
[9] Zhang L, Fan C, Hao W, Zhuang Y, Liu X, Zhao Y, et al. NSCs migration promoted and drug delivered exosomes-collagen scaffold via a bio-specific peptide for one-step spinal cord injury repair. Adv Healthc Mater 2021;10(8):2001896.
[10] Y Liu X, Chen C, Xu HH, Zhang Y, Zhong L, Hu N, et al. Integrated printed BDNF/collagen/chitosan scaffolds with low temperature extrusion 3D printer

accelerated neural regeneration after spinal cord injury. Regen Biomater 2021;8(6).
[11] Liu X, Kim JC, L Miller A, Waletzki BE, Lu L. Electrically conductive nanocomposite hydrogels embedded with functionalized carbon nanotubes for spinal cord injury. Nouv J Chim 2018;42(21):17671–81.
[12] Huang F, Chen T, Chang J, Zhang C, Liao F, Wu L, et al. A conductive dual-network hydrogel composed of oxidized dextran and hyaluronic-hydrazide as BDNF delivery systems for potential spinal cord injury repair. Int J Biol Macromol 2021;167:434–45.
[13] Zhang K, Li J, Jin J, Dong J, Li L, Xue B, et al. Injectable, anti-inflammatory and conductive hydrogels based on graphene oxide and diacerein-terminated four-armed polyethylene glycol for spinal cord injury repair. Mater Des 2020;196:109092.
[14] Yang B, Wang PB, Mu N, Ma K, Wang S, Yang CY, et al. Graphene oxide-composited chitosan scaffold contributes to functional recovery of injured spinal cord in rats. Neural Regen Res 2021;16(9):1829–35.
[15] Xu C, Chang Y, Wu P, Liu K, Dong X, Nie A, et al. Two-dimensional-germanium phosphide-reinforced conductive and biodegradable hydrogel scaffolds enhance spinal cord injury repair. Adv Funct Mater 2021;31(41):2104440.
[16] Kiyotake EA, Martin MD, Detamore MS. Regenerative rehabilitation with conductive biomaterials for spinal cord injury. Acta Biomater 2020;139:43–6.
[17] Zhou L, Fan L, Yi X, Zhou Z, Liu C, Fu R, et al. Soft conducting polymer hydrogels cross-linked and doped by tannic acid for spinal cord injury repair. ACS Nano 2018;12(11):10957–67.
[18] Raynald B Shu, Liu XB, Zhou JF, Huang H, Wang JY, Sun XD, et al. Polypyrrole/polylactic acid nanofibrous scaffold cotransplanted with bone marrow stromal cells promotes the functional recovery of spinal cord injury in rats. CNS Neurosci Ther 2019;25(9):951–64.
[19] Wu C, Chen S, Zhou T, Wu K, Qiao Z, Zhang Y, et al. Antioxidative and conductive nanoparticles-embedded cell niche for neural differentiation and spinal cord injury repair. ACS Appl Mater Interfaces 2021;13(44):52346–61.
[20] Zhang P, Hölscher C, Ma X. Therapeutic potential of flavonoids in spinal cord injury. Rev Neurosci 2017;28(1):87–101.
[21] Schültke E, Kendall E, Kamencic H, Ghong Z, Griebel RW, Juurlink BHJ. Quercetin promotes functional recovery following acute spinal cord injury. J Neurotrauma 2003;20(6):583–91.
[22] Wang Y, Li W, Wang M, Lin C, Li G, Zhou X, et al. Quercetin reduces neural tissue damage and promotes astrocyte activation after spinal cord injury in rats. J Cell Biochem 2018;119(2):2298–306.
[23] Elashmawi IS, Ismail AM, Abdelghany AM. The incorporation of Polypyrrole (PPy) in CS/PVA composite films to enhance the structural. Optical, and the electrical conductivity. Polym Bull 2022. https://doi.org/10.1007/s00289-022-04611-6.
[24] Mukhopadhyay P, Maity S, Chakraborty S, Rudra R, Ghodadara H, Solanki M, et al. Oral delivery of Quercetin to diabetic animals using novel pH responsive carboxypropionylated chitosan/alginate microparticles. RSC Adv 2016;6:73210–21. https://doi.org/10.1039/c6ra12491g.
[25] Sripriya R, Kumar R. A novel enzymatic method for preparation and characterization of collagen film from swim bladder of fish Rohu (Labeorohita). Food Nutr Sci 2015;6(15):1468.
[26] Kolesnichenko IV, Goloverda GZ, Kolesnichenko VL. A versatile method of ambient-temperature solvent removal. Org Process Res Dev 2020;24(1):25–31.
[27] Hung PS, Kuo YC, Chen HG, Chiang HH, Lee OK. Detection of osteogenic differentiation by differential mineralized matrix production in mesenchymal stromal cells by Raman spectroscopy. PLoS One 2013;8(5):e65438. https://doi.org/10.1371/journal.pone.0065438.
[28] Turczyn R, Krukiewicza Katarzyna K, Katunin A, Srokac J, Sul P. Fabrication and application of electrically conducting composites for electromagnetic interference shielding of remotely piloted aircraft systems. Compos Struct 2020;232:111498.
[29] Ly A, Luo Y, Cavaillès G, Olivier MG, Debliquy M, Lahem D. Ammonia sensor based on vapor phase polymerized Polypyrrole. Chemosensors 2020;8(2):38.
[30] Catauro M, Papale F, Bollino F, Piccolella S, Marciano S, Nocera P, et al. Silica/quercetin sol–gel hybrids as antioxidant dental implant materials. Sci Technol Adv Mater 2015;16(3):035001.
[31] Sun TW, Zhu YJ, Chen F. Hydroxyapatite nanowire/collagen elastic porous nanocomposite and its enhanced performance in bone defect repair. RSC Adv 2018;8(46):26218–29.
[32] Sidhu GK, Kumar R. Study the structural and optical behaviour of conducting polymer based nanocomposites: ZrO2-Polypyrrole nanocomposites. IOP Conf Ser Mater Sci Eng 2018;360(1).
[33] Lucida H, Pradana R, Febriyenti, Rahmatika L. Preparation of quercetin nanocrystals by planetary ball mill to increase the solubility and the dissolution profile. Pharm Times 2016;8(18):53–8.
[34] Vinothini K, Rajendran NK, Ramu A, Elumalai N, Rajan M. Folate receptor targeted delivery of paclitaxel to breast cancer cells via folic acid conjugated graphene oxide grafted methyl acrylate nanocarrier. Biomed Pharmacother 2019;110:906–17.
[35] Blanco MJD, Montoya MR, Palma A, Paz MVD. Thermogravimetry applicability in compost and composting research: a review. Appl Sci 2021;11(4):1692.
[36] Koch D, Rosoff W, Jiang J, Urbach J. Strength in the periphery: growth cone biomechanics and substrate rigidity response in peripheral and central nervous system neurons. Biophys J 2012;102:452–60.
[37] Pampaloni NP, Lottner M, Giugliano M, Matruglio A, D'Amico F, Prato M, et al. Single-layer graphene modulates neuronal communication and augments membrane ion currents. Nat Nanotechnol 2018;13:755.
[38] Holder AJ, Badiei N, Hawkins K, Wright C, Williams PR, Curtis DJ. Control of collagen gel mechanical properties through manipulation of gelation conditions near the sol–gel transition. Soft Matter 2018;14(4):574–80.
[39] Weisel JW. The mechanical properties of fibrin for basic scientists and clinicians. Biophys Chem 2004;112:267–76.
[40] Curtis DJ, Williams PR, Badiei N, Campbell AI, Hawkins K, Evans PA, et al. A study of microstructural templating in fibrin–thrombin gel networks by spectral and viscoelastic analysis. Soft Matter 2013;9:4883–9.
[41] Chougule MA, Pawar SG, Godse PR, Mulik RN, Sen S, Patil VB. Synthesis and characterization of Polypyrrole (PPy) thin films. SNL 2011;1:6–10.
[42] Singh D, Rawat MS, Semalty A, Semalty M. Quercetin-phospholipid complex: an amorphous pharmaceutical system in herbal drug delivery. Curr Drug Discov Technol 2012;9(1):17–24.
[43] Rodríguez-Félix F, Del-Toro-S'anchez CL, Cinco-Moroyoqui FJ, Juarez J, Ruiz-Cruz S, Lopez-Ahumada GA, et al. Preparation and characterization of quercetin-loaded zein nanoparticles by electrospraying and study of *in-vitro* bioavailability. J Food Sci 2019;84(10):2883–97.
[44] Rao CRK, Muthukannan R, Jebin JA, Raj T, Vijayan M. Synthesis and properties of Polypyrrole obtained from a new Fe (III) complex as oxidizing agent. Indian J Chem 2013;52A:744–8.
[45] Wang X, Fu Y, A Botchway BO, Zhang Y, Zhang Y, Jin T, et al. Quercetin can improve spinal cord injury by regulating the mTOR signaling pathway. Front Neurol 2022;13:905640.
[46] Mehany ABM, Belal A, Santali EY, Shaaban S, Abourehab MAS, El-Feky OA, et al. Biological effect of quercetin in repairing brain damage and cerebral changes in rats: molecular docking and in vivo studies. BioMed Res Int 2022;26:8962149.
[47] Jang J, Lee S, Oh HJ, Choi Y, Choi JH, Hwang DW, et al. Fluorescence imaging of in vivo miR-124a-induced neurogenesis of neuronal progenitor cells using neuron-specific reporters. EJNMMI Res 2016 Dec;6(1):38. https://doi.org/10.1186/s13550-016-0190-y.
[48] Messing A, Brenner M. GFAP: functional implications gleaned from studies of genetically engineered mice. Glia 2003;43:87–90. https://doi.org/10.1002/glia.10219.
[49] Wu X, Yoo S, Wrathall JR. Real-time quantitative PCR analysis of temporal–spatial alterations in gene expression after spinal cord contusion. J Neurochem 2005;93:943–52. https://doi.org/10.1111/j.1471-4159.2005.03078.x.